Articles

X-ray Structure of Two Complexes of the Y143F Flavocytochrome b_2 Mutant Crystallized in the Presence of Lactate or Phenyl Lactate[†,‡]

Mariella Tegoni,*[,§] Simone Begotti,[||] and Christian Cambillau[§]

Laboratoire de Cristallographie et Cristallisation des Macromolécules Biologiques, URA-1296 CNRS, 31 Chemin Joseph Aiguier, 13402 Marseille Cedex 20, France, and Istituto di Scienze Biochimiche, Università di Parma, Viale delle Scienze, 43100 Parma, Italia

Received February 14, 1995; Revised Manuscript Received April 24, 1995[⊗]

ABSTRACT: Flavocytochrome b_2 is a flavohemo enzyme localized in the intermembrane space of yeast mitochondria, where it catalyzes the electron transfer from its substrate, L-lactate, to cytochrome *c*. We have obtained crystals of a flavocytochrome b_2 mutant, Y143F, which are isostructural with those of the native recombinant enzyme [Tegoni, M., & Cambillau, C. (1994) *Protein Sci. 3*, 303−314]. These crystals were grown under similar conditions to those used to obtain the recombinant enzyme, but in the presence of phenyl lactate or lactate. We report here on the structural analysis of the two complexes of flavocytochrome b_2 with the reaction products at 2.9 Å resolution. In both structures, the Phe143 phenyl ring keeps the same position as that of the phenolic ring of Tyr143 in both the native recombinant and in the native wild-type enzymes. The product of the reaction, phenyl pyruvate or pyruvate, is present at the active site of both subunits, and not only in subunit 2 as observed in the wild-type structure [Xia, Z.-X., & Mathews, F. S. (1990) *J. Mol. Biol. 212*, 837−863]. The number of interactions between the FMN and the heme domain is considerably lower in the Y143F mutant than in the native proteins. The latter finding strongly supports the hypothesis that the main role of Tyr143 in the native protein probably consists in establishing a hydrogen bond with the heme [Xia, Z.-X., & Mathews, F. S. (1990) *J. Mol. Biol. 212*, 837−863]. This interaction appears to be essential for the two domains to approach each other suitably so that the intramolecular electron transfer can occur.

In the intermembrane space of yeast mitochondria, flavocytochrome b_2 (L-lactate:cytochrome *c* oxidoreductase, EC 1.1.2.3) catalyzes the electron transfer from L-lactate to cytochrome *c* (Pajot & Claisse, 1974). The functional protein is a tetramer (4 × 58 kDa) (Baudras, 1972; Jacq & Lederer, 1974), and each subunit carries a FMN[1] and a b_5-like heme (Baudras, 1962; Guiard et al., 1974). The kinetic and thermodynamic properties of this protein purified from *Saccharomyces cerevisiae* and *Hansenula anomala* have previously been characterized (Capeillère-Blandin et al., 1975, 1982; Iwatsubo et al., 1977; Pompon et al., 1980; Labeyrie, 1982; Tegoni et al., 1984, 1986).

The protein from *S. cerevisiae* has been cloned (Guiard, 1985; Reid et al., 1988) and expressed in *Escherichia coli* (Black et al., 1989). The kinetic behavior of the wild-type and that of the native recombinant protein are comparable (Reid et al., 1988; Dubois et al., 1990; Miles et al., 1992).

The three-dimensional structure of *S. cerevisiae* (Xia & Mathews, 1990) and that of the recombinant flavocytochrome b_2 (Tegoni & Cambillau, 1994a) are very similar. The two subunits present in the asymmetric unit are structurally nonequivalent: in subunit 1, the heme and the FMN domains are both visible in the electron density map, whereas in subunit 2 only the FMN domain is visible, probably because the heme domain is either disordered or may have multiple conformations (Figure 1). Moreover, in the *S. cerevisiae* flavocytochrome b_2 structure, a molecule of the reaction product, pyruvate, is visible only at the FMN site of subunit 2 (Figure 3B); it is replaced by water molecules in subunit 1 (Xia et al., 1987; Xia & Mathews, 1990).

A mechanism possibly accounting for the catalytic oxidation of L-lactate has been proposed (Lederer & Mathews, 1987; Lederer, 1992), and putative roles have been described for the various amino acids at the FMN site and binding pyruvate (Figure 2). In particular, Tyr143 OH participates in the orientation of the substrate by hydrogen-bonding the carboxylate group in subunit 2 (Figure 3B). In subunit 1, where there is no pyruvate, Tyr143 OH is at the interface between the FMN domain and the heme domain and hydrogen-bonded to the A propionate of the heme (2.4 Å) (Figure 3A). Due to its localization, Tyr143 is thought to be possibly involved in the electron transfer from the FMN to the heme b_2, either as an electron relay via the aromatic π-bonds of its side chain or by participating in an interaction which is fundamental to the recognition between the two

[†] This work was supported by the CNRS-IMABIO programme and the PACA region.

[‡] The coordinates have been deposited with the Protein Data Bank, accession numbers 1LDC and 1LCO.

* Corresponding author. E-mail: tegoni@lccmb.cnrs-mrs.fr.

[§] CNRS.

[||] Università di Parma.

[⊗] Abstract published in *Advance ACS Abstracts,* June 15, 1995.

[1] Abbreviations: flavinmononucleotide, FMN; mutant Tyr143→Phe143, Y143F; complex with phenyl pyruvate, Y143F-Ppyr; complex with pyruvate, Y143F-pyr; phenyl pyruvate, Ppyr; pyruvate, pyr.

0006-2960/95/0434-9840$09.00/0

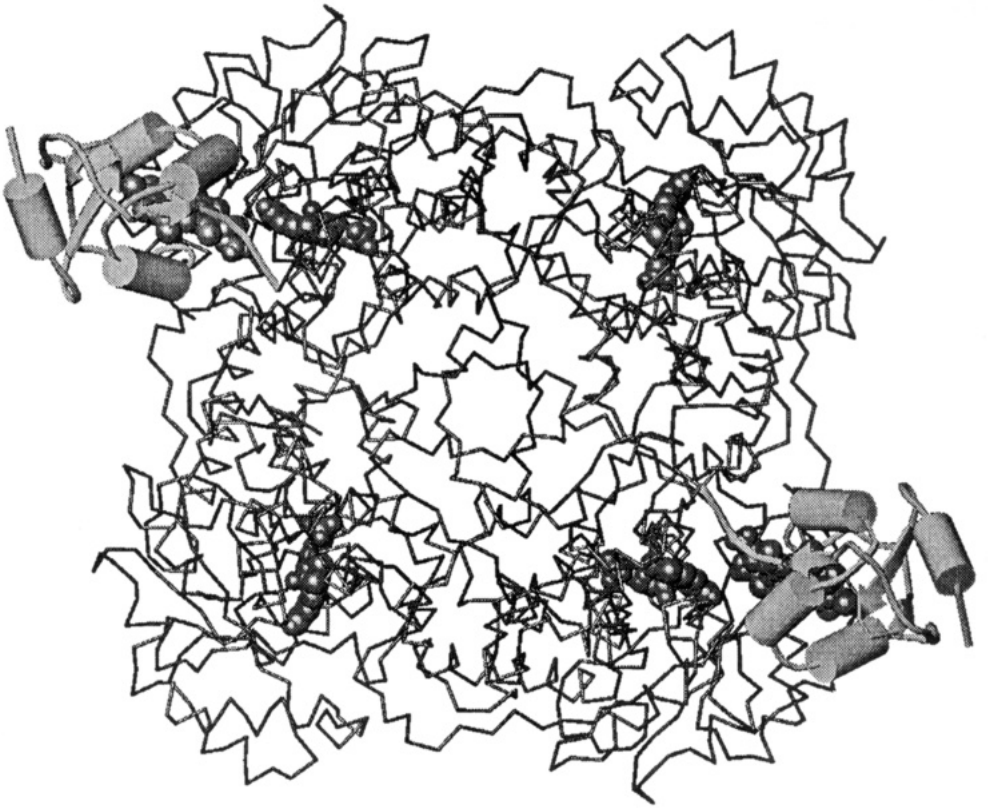

FIGURE 1: Ribbon view of crystalline flavocytochrome b_2 tetramer. The heme domains are represented according to their secondary structure type (arrows and cylinders). The prosthetic groups are shown using CPK representation.

domains. In fact, it has been suggested that the approach of the FMN and the heme domains may be one of the decisive factors on which the intramolecular electron transfer in flavocytochrome b_2 depends [dynamic control hypothesis (Miles et al., 1992; Tegoni & Cambillau, 1994a)].

Among the various site-directed mutants of flavocytochrome b_2 which have been produced with the view of probing the active site (Reid et al., 1988; Black et al., 1989), the mutant Tyr143→Phe was designed to abolish the hydrogen bonds with the substrate carboxyl end and with the heme propionate and to test the role of the OH side chain in the native protein. The kinetic behavior of this mutant, expressed in *E. coli*, has been described (Reid et al., 1988; Miles et al., 1992; Rouvière-Fourmy et al., 1994). The results show in particular that Tyr143 OH plays a crucial role in the electron transfer from FMN to the heme, since this step decreased in rate 20-fold and became the limiting step in the whole mechanism (Table 1) (Miles et al., 1992), and in the affinity of the enzyme for the substrate which is also significantly decreased (K_{diss} L-lactate 4 times higher; Table 1) (Rouvière-Fourmy et al., 1994).

Here we present the first X-ray structures (2.9 Å) of a mutant of flavocytochrome b_2. The Y143F mutant is crystallized in the presence of either its physiological substrate, lactate, or a poor substrate, phenyl lactate. The choice of phenyl lactate in this study was dictated by the need of unambiguously identify the reaction product at both active sites, using the phenyl group as a marker. The structural data will be discussed in terms of the effect of the mutation on the electron transfer, the mobility, and the dynamic behavior of the heme domain. A preliminary report of this study has been presented elsewhere (Tegoni & Cambillau, 1994b).

MATERIALS AND METHODS

Protein Growth and Purification. Plasmid-bearing *E. coli* were grown at 37 °C in Luria broth supplemented with ampicillin at 100 μg/mL; cell lysis and the first purification steps were carried out as described by Black et al. (1989) with minor modifications. Flavocytochrome b_2 was purified using the procedure described by Labeyrie et al. (1978). The affinity chromatography on Sepharose 4B-oxalate linked was omitted, since the recombinant protein generally shows an optimal degree of purity after hydroxylapatite fractionation. The standard ferricyanide reductase activity was checked as described in Labeyrie et al. (1978). The purified protein showed a single SDS−PAGE band.

Crystallization. Crystals of Y143F flavocytochrome b_2 (25 mg/mL) were obtained using the vapor diffusion technique in the presence of PEG 4000 (10−12% w/w) and 50 mM MES buffer, pH 5.5, at 20 °C. Crystals suitable for X-ray analysis were obtained in the presence of sodium D,L-phenyl lactate (20 mM), and sodium D,L-lactate (10 mM). These crystals are isomorphous with those of the wild-type flavocytochrome b_2 from *S. cerevisiae* (Xia & Mathews, 1990) and of the *E. coli* recombinant native protein (Tegoni & Cambillau, 1994), with space group $P3_221$ and cell dimensions $a = b = 164.5$ Å and $c = 114.0$ Å.

Data Collection, Structure Refinement, and Analysis. Data were collected at a nominal resolution of 2.6 Å on a 18 cm Mar-Research Imaging Plate detector placed on a Rigaku RU200 rotating anode working at 40 kV × 85 mA. Statistics on the various data collections are given in Table 2. The crystal detector distance was 14 cm. Data were collected at 16 °C, with 1° of oscillation and a total rotation angle of 60°. The exposure time was 1200 s/deg. Integration was performed using the MOSFLM package (Leslie, A., MRC,

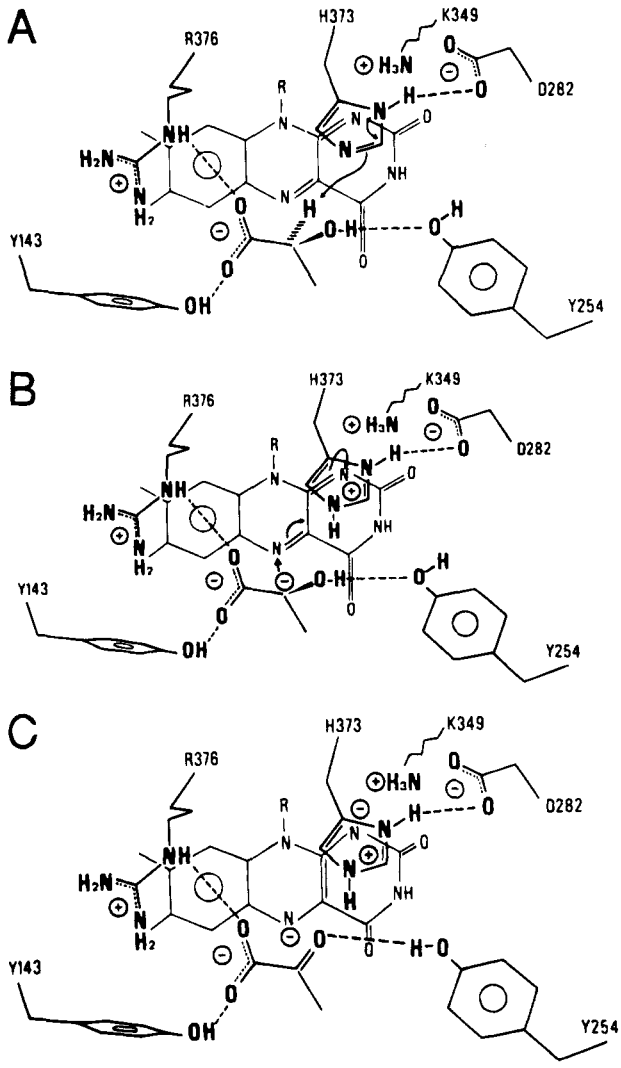

FIGURE 2: Proposed mechanism of L-lactate oxidation by flavocytochrome b_2. Reproduced with permission from Lederer (1992).

Cambridge, U.K.). Although the data were collected at a nominal resolution of 2.6 Å, we discarded the data in the 2.6−2.9 Å shell, due to their poor quality.

Structure refinement was performed using X-PLOR (Brünger, 1988). The initial model contained subunits 1 and 2. The atomic coordinates used were those of the recombinant native protein. Four cycles of X-PLOR simulated annealing were performed: prep stage, 0.5 ps cool stage at 300 K, final stage and *B* refinement. These were followed by four stages of minimization procedure. Visual inspection and manual refitting were performed between each cycle with the TURBO-FRODO software program on Silicon Graphics stations (Roussel & Cambillau, 1991). After the first cycle of refinement, the $2F_o - F_c$ and $F_o - F_c$ maps were computed with a cushion of 30 Å around the molecule (see below). No electron densitiy was detected for the heme domain of subunit 2 or the protease-sensitive loops. Peaks of negative electron density were clearly visible in the $F_o - F_c$ maps at the position of the former OH of tyrosines 143 (Figure 4A,B). The side chain was manually changed into phenylalanine; it did not move significantly during further refinements. Positive electron density was visible in both active sites. The reaction products, phenyl pyruvate or pyruvate, were fitted into the density at this stage. Water molecules were added when visible, throughout the refinement procedure. Minor rebuildings were necessary with both complexes of Y143F mutant and were restricted to removing a few amino acids at the N-terminal and at both ends of the protease-sensitive region: the peptide chain started to fit the density at residues 10 and 102 in subunits 1 and 2, respectively, for both complexes; the disordered regions range from 299 to 320 in subunit 1 of Y143F-Ppyr and Y143F-Pyr, and from 297 to 315 and 297 to 324 in subunit 2 for Y143F-Ppyr and Y143F-pyr, respectively. A further cycle of refinement was carried out at the end of the refinement procedure without ligands, and the resulting maps did not differ significantly from the final refinement maps obtained with them. The final *R* factors were 18.6% and 19.5% (for 7075 and 7077 atoms, including 165 and 140 water molecules) with Y143F-Ppyr and Y143F-pyr, respectively, in the 6.0−2.9 Å resolution range, including all the data with $(I/\sigma I) > 1$ (Table 2).

Structure and domain alignments were performed with the RIGID option of the TURBO-FRODO package. Structure analysis was carried out using the TURBO-FRODO graphics package for *B* factors and deviation plots, distances, and angle measurements. The views in Figure 1 and those of the structure were plotted from TURBO-FRODO PostScript outputs (Roussel & Cambillau, 1991). *B* factor statistics and bond and angle deviations from the ideal and crystal packing analysis were performed with X-PLOR (Brünger, 1988).

RESULTS AND DISCUSSION

Structure Description

Domain Architecture and Overall Structure. The structure of the mutant enzyme in both complexes closely resembles those of *S. cerevisiae* (Xia & Mathews, 1990) and of the recombinant flavocytochrome b_2 (Tegoni & Cambillau, 1994a) (Figure 1). The structure of the FMN and the heme domains have been previously described, and no electron density has been observed for the heme domain of subunit 2, which indicates that it must be disordered. Two fundamental findings made here on the structures of the Y143F complexes were that the phenyl ring of Phe143 keeps a position which is very similar to that of the phenolic ring of Tyr143 in the native recombinant structure and that the reaction products are also present in subunit 1.

The final stereochemistry was satisfactory, as indicated by the PROCHECK Ramachandran plot (Morris et al., 1992) (Figure 5A,B): the few amino acids outside the allowed regions on the Ramachandran plot were at the N-terminal (23A) and C-terminal (493A), in the hinge region, connecting the heme and the FMN domain (102A, 103B, 149B, 150B), and at Gln377 in both subunits.

Except for the nonvisibility of the heme domain in subunit 2, the two subunits were found to also have very similar conformations. After superimposing the FMN domains, the mean deviation of the Cα was 0.36 and 0.42 Å with Y143F-Ppyr and Y143F-pyr, respectively (Table 3). The deviation from planarity of the FMN groups was similar, since values ranging between 172° and 174° were obtained for the butterfly angle between pyrimidine and benzenoid rings in the two subunits in both the complexes. These values are quite comparable to those found previously in the native (Xia & Mathews, 1990) and in the recombinant structures (172° and 173° in subunits 1 and 2, respectively).

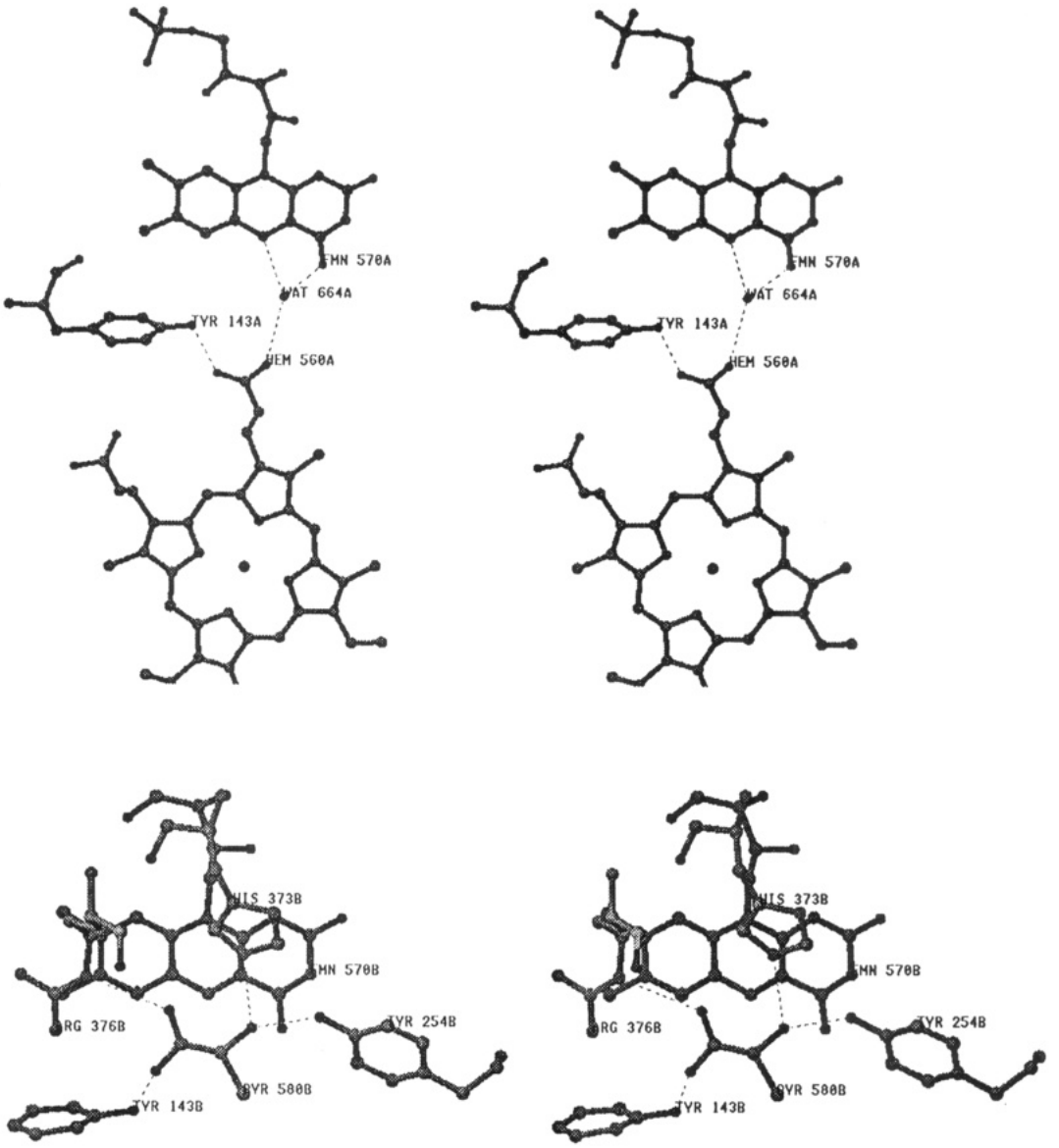

FIGURE 3: Stereoview of Tyr143 and its interactions in wild-type flavocytochrome b_2 structure. (A, top) Subunit 1; (B, bottom) subunit 2.

Table 1: Kinetic Parameters of Native Recombinant and Y143F Mutant

			k_{cat} L-lactate (s^{-1})		K_M L-lactate (mM)		
	k_{max} FMN (s^{-1})	k_{max} heme (s^{-1})	$Fe(CN)_6^{3-}$	cyt *c*	$Fe(CN)_6^{3-}$	cyt *c*	K_{diss} L-lactate (mM)
native[a]	604 ± 60	445 ± 50	400 ± 10	103 ± 5	0.49 ± 0.05	0.24 ± 0.04	
recombinant Y143F[a]	735 ± 80	21 ± 2	400 ± 30	11 ± 1	2.90 ± 0.23	0.23 ± 0.03	
native[b]	144 ± 4			196 ± 12		0.36 ± 0.02	0.46 ± 0.23
recombinant Y143F[b]	310 ± 19			40 ± 8		0.37 ± 0.16	2.10 ± 1.05

[a] Tris-HCl 10 mM, $I = 0.1$ with NaCl, pH 7.5, 25 °C. Miles *et al.* (1992). [b] 100 mM Na^+/K^+ phosphate buffer, 1 mM EDTA, pH 7.0 ($I = 0.22$), 5 °C. Rouvière-Fourmy *et al.* (1994). k_{cat} are expressed in electron transferred per second per mole of enzyme.

The average *B* factor values were only slightly higher than those of the native recombinant protein. Those of the products, phenyl pyruvate and pyruvate, were about twice the average value obtained on the protein (Table 4). This is in line with what has been observed in the native structure (Xia & Mathews, 1990) but contrasts with the data on the native recombinant structure, where the covalent linkage of sulfite with the N5 of the flavin may account for the low *B* factor observed (Tegoni & Cambillau, 1994a). The high *B* factors of phenyl pyruvate and pyruvate in the complex with the Y143F mutant may be attributable either to a high degree of mobility or to a lack of full occupancy of the active site by these molecules. The distribution of the *B* factor values along the polypeptidic chain was similar in the two structures analyzed: these values were particularly high in the heme domain (residues 10A−100A), at the N and C-termini of both FMN domains, close to the disordered regions, and around residue 400 in both subunits. As in the native structure, the presence of the heme domain in subunit 1 as well as the large number of packing constraints involving

Table 2: Data Collection and Final Refinement Statistics of Mutant Y143F Flavocytochrome b_2

	Y143F-Ppyr	Y143F-pyr
(A) Data Collection Statistics		
resolution range (Å)	100−2.9	100−2.9
number of measured reflections	263 169	156 473
number of independent reflections	35 569	32 412
data completion 100−2.9 Å	87%	80%
R_{sym} (all reflections)	13.0%	15%
(B) Final Refinement Statistics		
resolution range (Å)	6−2.9	6−2.9
total number of atoms	7077	6963
water molecules	165	141
R factor	18.6%	19.5%
root mean square deviations from ideal values		
bonds (Å)	0.010	0.010
angles (deg)	3.50	3.70

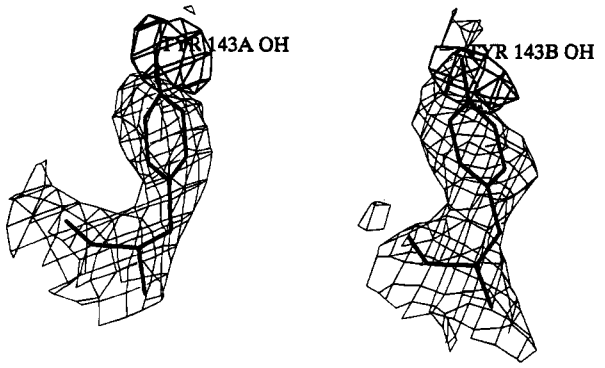

FIGURE 4: Views of the initial electron density maps, ($2F_o - F_c$) (thin lines), and negative ($F_o - F_c$) (thick lines) centered around OH atom of Tyr143 in subunit 1 (A, left) and in subunit 2 (B, right) of the Y143F mutant in complex with phenyl pyruvate.

this subunit may explain why markedly lower B factors were obtained in the case of the FMN domain of subunit 1 in comparison with those of subunit 2 (Table 4). The heme domain of both complexes of Y143F mutant has conspicuously higher B factors than those of the native structure, possibly because this domain may be more mobile. The mean deviation of the heme group was large (1.02 Å) in the complex with phenyl pyruvate (Table 3). This striking difference was probably due to steric hindrance between the phenyl pyruvate molecule and the heme (see further), which is in fact absent in the complex with pyruvate (0.41 Å, Table 3) and in the native recombinant.

The Active Sites

The Y143F-Ppyr Complex. The first difference Fourier ($F_o - F_c$) showed the existence of an elongated patch of electron density close to the FMN of subunit 1. This density peak was clearly different from a cluster of water molecules. A phenyl ring nicely fits into the wider part of the electron density region, and a three carbon atom moiety may account for the thinner part. The mutant Y143F has been proved to be catalytically competent, however poorly, with respect to phenyl lactate (see below); the reaction product, phenyl pyruvate, was therefore modeled into the electron density map and refined (Figure 6A). In subunit 2, a high electron density peak was also present in an equivalent position. This density region was less continuous, however, than that observed in subunit 1, and phenyl pyruvate was therefore added at later stages in the refinement procedure. In the final model, phenyl pyruvate is present in both subunits, but better defined in subunit 1 (Figure 6A,B). The B factors of phenyl pyruvate in subunit 2 are also larger than those obtained in the case of the same molecule in subunit 1 (Table 4).

Like pyruvate in the wild-type structure, the aliphatic part of phenyl pyruvate is parallel to the flavin ring on its *si* side. As was to be expected in the case of such a different molecule, however, the interactions involving phenyl pyruvate at the active site were found to differ greatly from those involving pyruvate in the structure of the wild-type protein. The phenyl pyruvate molecule is tilted (Figure 7A) as compared with pyruvate: the carboxyl end is then directed toward the FMN and the phenyl part toward the heme domain (Figure 8A). Several hydrophobic interactions and few hydrogen bonds hold phenyl pyruvate in its binding site. Phe143, Ala198 (and Leu199 in subunit 2), Leu230, and the heme group in subunit 1 surround the phenyl ring (Figure 8A,B). The O1B atom of carboxyl is hydrogen-bonded to Tyr254 OH atom and to His373 NE2 atom, and the O2 atom interacts with NH2 atom of Arg376. O1B is the atom located nearest to the FMN atom N5, only 3.4 and 3.1 Å apart in subunits 1 and 2, respectively. Furthermore, atom O2, which needs to be close to the FMN N5 atom for catalysis to occur, is remote from this site (>4.0 Å) (Table 5A). This result may indicate either that the catalysis proceeds via a different reaction pathway or that the product rearranges its position drastically after the reaction, or both. To date, there is no evidence that any other kinetic mechanism may operate in this mutant (Reid et al., 1988; Miles et al., 1992; Rouvière-Fourmy et al., 1994). The catalytic activity of the Phe143 mutant enzyme with phenyl lactate is very poor, ca. 5% of its activity with lactate (not shown). This supports the hypothesis that a catalytically efficient complex between acceptor and donor (such as that which occurs in the native enzyme) must be formed only seldom. Moreover, the position of phenyl pyruvate diffused into a preformed crystal of the wild-type protein was superimposable on that of pyruvate at the active site (Mathews, personal communication). In our structure, the position of the product we observed might have been shifted from the position of the substrate during catalysis, possibly as the result of a rearrangement of the product after the catalytic event. The driving force underlying this reorientation of the phenyl pyruvate molecule might be the hydrophobic interactions involving the phenyl ring, as discussed below. One consequence of this reorientation of the phenyl ring is that propionate A of the heme group moves away out of the heme plane (Figure 8A).

The presence of a product as bulky as phenyl pyruvate in the active site is probably the reason for the large difference (1.02 Å) observed for the heme group between this and that of the native enzyme (Table 3). This also reflects the great intrinsic accessibility of the FMN site. These data, moreover, show for the first time that the active site in subunit 1, i.e., in the *closed* conformation of the flavocytochrome b_2 monomer, in which the heme domain is ordered, is able to accomodate the reaction product.

Y143F-pyr. In this complex, an isolated patch of electron density was again observed near the FMN site. This electron density patch was clearly visible in both subunits but was less clearly visible in subunit 2. This is in agreement with the data on the above mentioned structure, but not with the data published on the wild-type structure (Xia & Mathews,

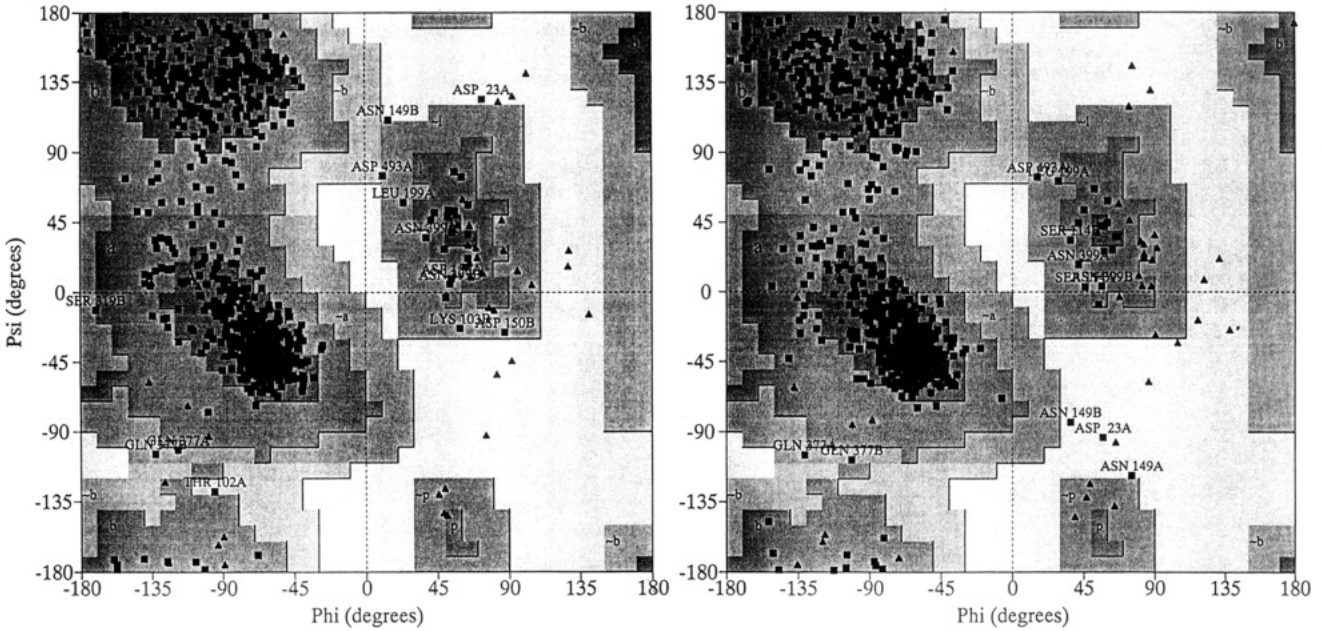

FIGURE 5: Ramachandran plot of the flavocytochrome b_2 crystallographic dimer after refinement. (A, left) Complex with phenyl pyruvate; (B, right) complex with pyruvate.

Table 3: Mean Deviation Å after Domain Structural Alignment between Subunit 1 and 2 of Y143F Mutant, between Y143F and Recombinant Flavocytochrome b_2

structures aligned with	domain compared	Cα	side chain
(A) Y143F-Ppyr			
FDHA/FDHB mutant	FDH	0.36	0.47
	FMN		0.83
	substrate		0.55
sub 1 mutant/rec	sub 1	0.28	0.51
	core	0.54	0.83
	heme		0.93
core mutant/rec	core	0.50	0.81
	heme		1.02
FDHA mutant/rec	core	0.75	0.84
	heme		0.93
	FDHA	0.22	0.43
	FMN A		0.21
FDHB mutant/rec	FDHB	0.29	0.48
	FMN B		0.25
(B) Y143F-pyr			
FDHA/FDHB mutant	FDH	0.42	0.45
	FMN		0.90
	substrate		1.82
sub 1 mutant/rec	sub 1	0.32	0.57
	core	0.61	0.88
	heme		0.53
core mutant/rec	core	0.50	0.83
	heme		0.41
FDHA mutant/rec	core	0.65	0.91
	heme		0.55
	FDHA	0.25	0.48
	FMN A		0.24
FDHB mutant/rec	FDHB	0.27	0.52
	FMN B		0.31

Table 4: Average *B* Factors (Main/Side Chain, Å^2) of Y143F Mutant and Recombinant Flavocytochrome b_2 Domains, Prosthetic Groups, and Inhibitor or Products

domain/group	native recombinant	Y143F-Ppyr	Y143F-pyr
sub 1 + sub 2	26/29	33/35	39/41
heme domain	62/64	75/71	81/73
FMN domain sub 1	18/20	22/24	30/31
FMN domain sub 2	26/29	34/35	39/41
heme group	41	52	73
FMN in sub 1	7	6	12
FMN in sub 2	15	21	32
sulfite sub 1/2	28/28		
product sub 1/2		50/68	65/50
solvent	42	51	51

1990). The patch of electron density, slightly elongated and almost flat, was compatible here with a three carbon molecule, either lactate or pyruvate. For the same reasons mentioned above, a molecule of pyruvate has been fitted into this density map and refined. Starting from equivalent positions, the orientation of pyruvate developed differently in the two subunits during the refinement (Figures 7B and 8C,D). In the final model, pyruvate is present at both the active sites, parallel to the FMN on the *si* side; as in the complex with phenyl pyruvate, pyruvate is more clearly defined in subunit 1 (Figure 6C,D). The *B* factors are given in Table 4. The position of pyruvate is close to that of wild-type in subunit 2, but the definition is poor. In subunit 1, the molecule is shifted by about 1.4 Å and tilted 90° (anticlockwise) in comparison with the position in the wild-type enzyme: the COO^- group is pointing down toward Arg289 and Phe143, and the O2 and CH3 atoms are pointing up toward the FMN C5α and C4α atoms, respectively (Figures 7B and 8C,D). Several hydrogen bonds are formed with the amino acids at the active site: in subunit 1, His373 NE2 and Arg376 NE atoms with atom O2, and Arg289 NH2 and Arg376 NH1 atoms with atom O1A, but there is an empty space opposite the O1B atom; in subunit 2, Tyr254 OH and His373 NE2 atoms with atom O2, Arg289 NH2, His373 NE2, and Arg376 NH2 atoms with atom O1A, and Arg289 NH1 and Arg376 NH2 atoms with atom O1B (Figure 8C,D and Table 5B). A single hydrophobic interaction with pyruvate is present in the wild-type, whereas C3 interacts with hydrophobic atoms belonging to the FMN ring in subunit 1 and with Ala198 and Leu286 in subunit 2, in the mutant. It looks just as if, in order to compensate for the loss of hydrogen-bonding to residue 143 in the mutant, pyruvate rotates in the active site to interact with Arg289, thus reinforcing the O1A atom hydrogen-bonding and producing new hydrophobic interactions with the atoms of

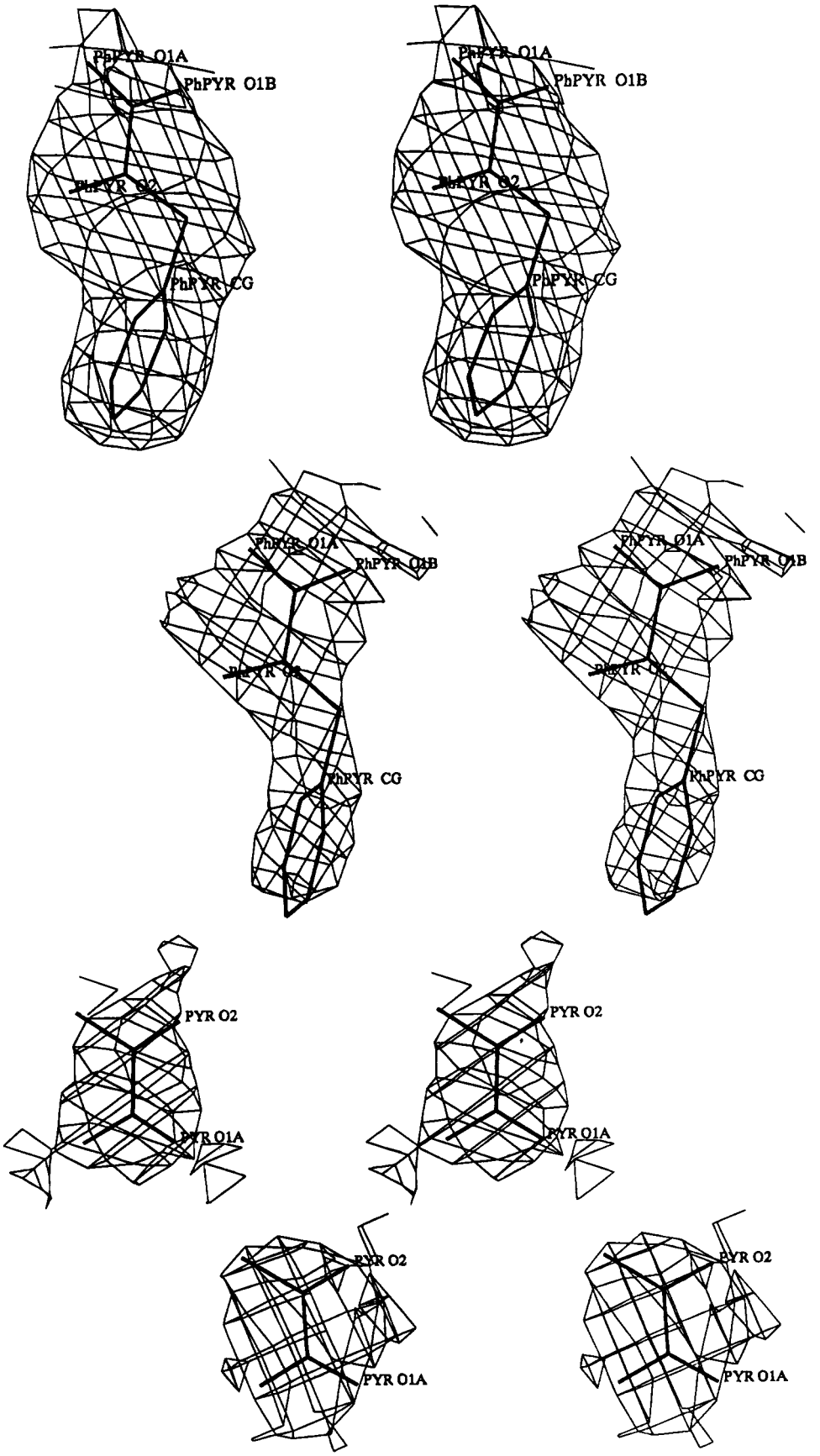

FIGURE 6: Stereoviews of the electron density maps ($2F_o - F_c$) of phenyl pyruvate in subunit 1 (A, top) and in subunit 2 (B, second from top) of the Y143F mutant and of pyruvate in subunit 1 (C, second from bottom) and in subunit 2 (D, bottom) of the Y143F mutant.

the FMN ring. The number of hydrogen bonds is equivalent to that present in the wild-type in the final position of pyruvate, but two additional hydrophobic interaction are formed. The O2 pyruvate atom is slightly closer to the N5 atom of the FMN but does not interact with Tyr254 OH (Table 5B).

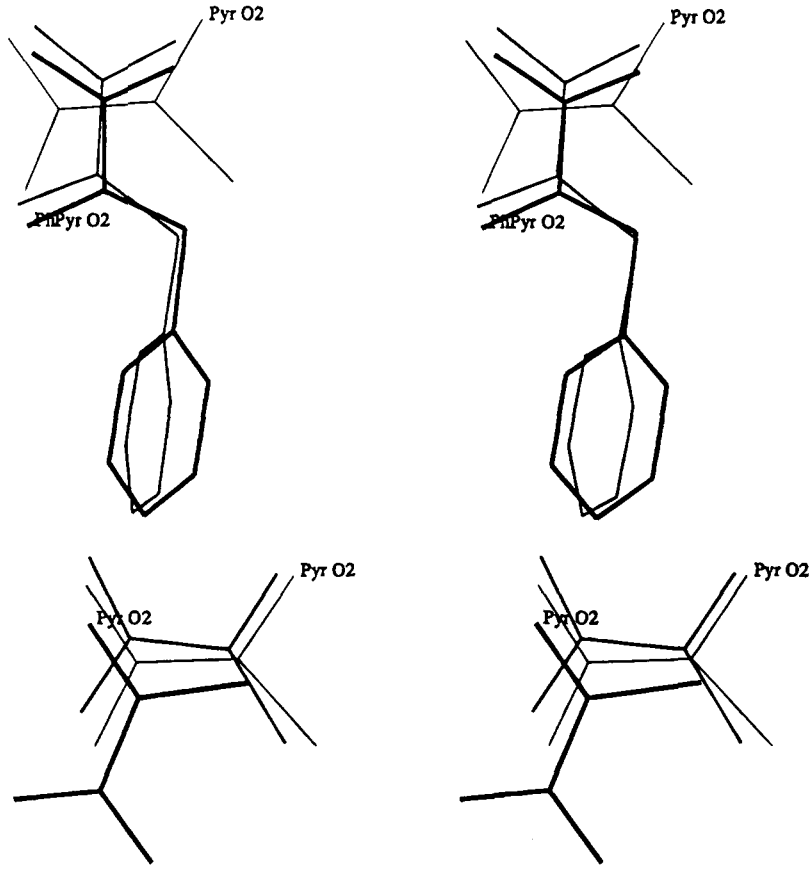

FIGURE 7: Plot of phenyl pyruvate (A, top) or pyruvate (B, bottom) in the Y143F mutant of flavocytochrome b_2 compared with pyruvate of the wild-type enzyme visible in subunit 2 (thick to thin lines: subunit 1, subunit 2, subunit 2 of the wild-type). The subunits are aligned on the flavin domain.

Depending on the experimental conditions, the rate of reduction of the FMN by L-lactate in the mutant has been found to be 1.2 or 2 times faster than that of the native structure (Table 1). This difference cannot be easily explained on the basis of the structural analysis of the Y143F mutant active site. The affinity of this mutant for L-lactate is about one-fourth that of the native enzyme (Table 1). This lower affinity has been attributed to the loss of the hydrogen bond between Tyr143 OH and the carboxylate of L-lactate, and this is confirmed here by the results of the X-ray analysis. The possibility that a weak polar interaction might occur on the contrary, between the carboxylate of L-lactate and the aromatic ring of Phe143, mentioned by Rouvière-Fourmy et al. (1994), now looks quite unrealistic on the basis of the three-dimensional structure.

Comparison with the Native Recombinant Structure

The FMN Domain and the Heme Domain. After rigid body fitting of the overall (mutant and native) molecules, superimposing the FMN domains yielded a mean deviation of ca. 0.22−0.29 Å; the heme domain was found to have slightly moved, giving a mean deviation of 0.65−0.75 Å (Table 3A,B). Performing a rigid body fitting of the heme domain separately gave a slightly closer fitting superimposition with a mean deviation of 0.5 Å. Upon making comparisons between the recombinant and wild-type flavocytochrome b_2, we previously described the rigid-body rotation of the heme domain with respect to the flavin domain (Tegoni & Cambillau, 1994a). In the Y143F mutant, the heme domain displays a movement similar to this one, but it is of smaller amplitude. Aligning of the isolated heme domain results in a satisfactory superimposition of the heme group in the Y143F-pyr (mean deviation 0.41 Å); whereas, in the complex with phenyl pyruvate, the heme is deeper in its pocket and rotated. Satisfactory superimposition was obtained by moving the heme of the mutant 0.2 Å (direction C → D; B → A, using the nomenclature of the heme pyrroles system) and rotating it 5° (direction B → A → D → C, nomenclature as before).

Prosthetic Groups: Relative Orientation and Distances. In our comparisons with the native recombinant structure, some differences are found in the position and orientation of the prosthetic groups. The mean deviation of the ring atoms of the FMN is 0.25 Å in the case of both subunits; the deviation is slightly larger for the ribityl chain and the N5. The latter effect is probably due to the attraction exerted by sulfite covalently linked in the recombinant structure (Tegoni & Cambillau, 1994a).

In comparison with the structure of the wild-type enzyme, the heme group in Y143F-Ppyr is tilted 8° and the propionate A is turned down toward the heme domain instead of being extended toward the FMN domain. This movement is absent in the native recombinant and in Y143F complexed with pyruvate; as mentioned above, it may result from steric hindrance, since in Y143F-Ppyr the A propionate extending toward the FMN domain would actually result in a clash with the phenyl ring of the phenyl pyruvate.

A general movement of all the amino acids involved in the catalysis is observed in the active site: the side chains of Asp 282, Arg376, and Phe/Tyr143 are significantly shifted

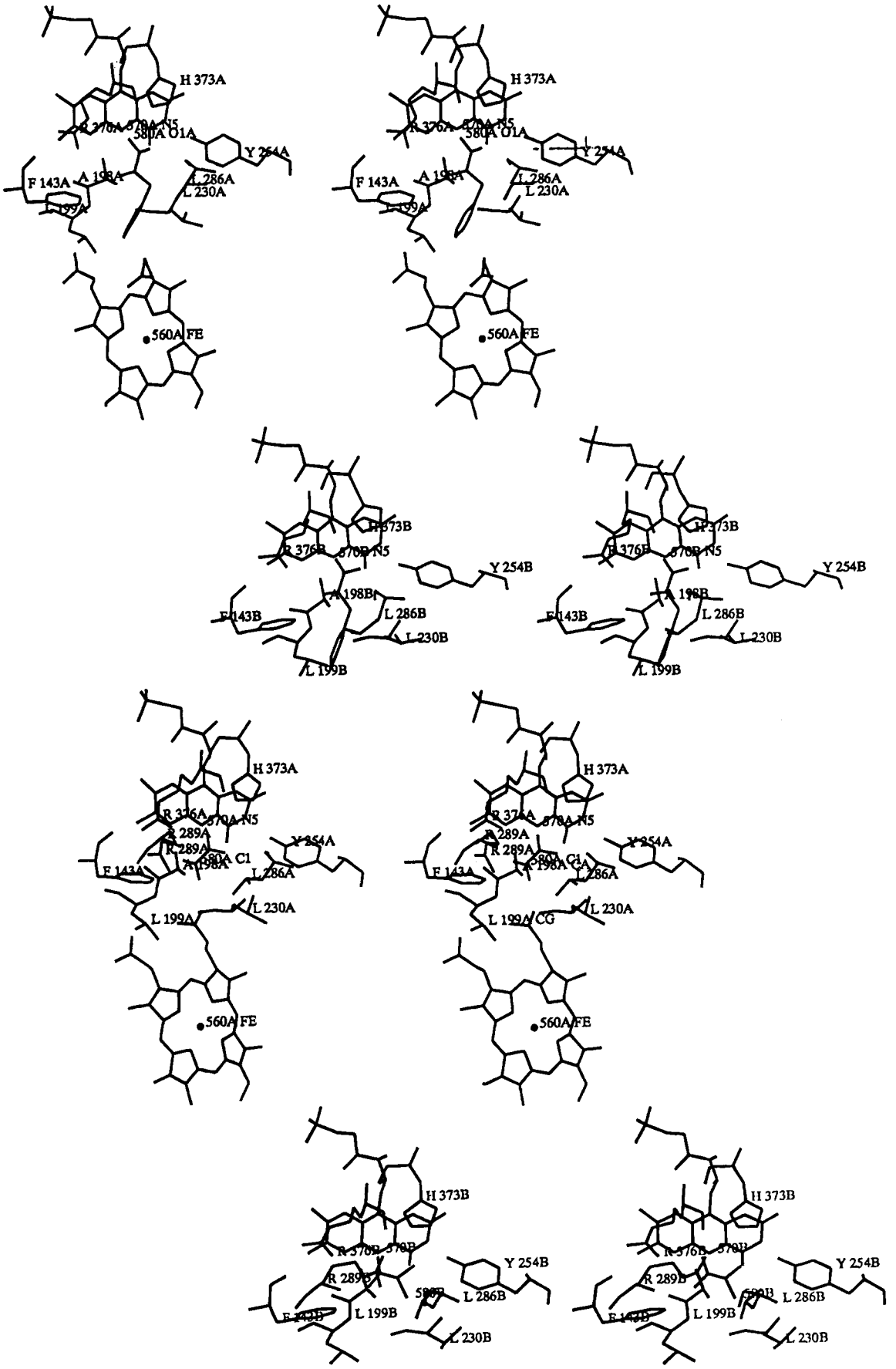

FIGURE 8: Stereoviews of phenyl pyruvate [(A, top) Subunit 1; (B, second from top) subunit 2] or pyruvate [(C, second from bottom) subunit 1; (D, bottom) subunit 2] bound in the active site of Y143F flavocytochrome b_2 mutant.

from the positions they assume in the recombinant enzyme (0.7 Å).

The edge-to-edge distance between the heme (C2A) and the FMN (N5) is 11.0 and 10.4 Å in the case of Y143F-

Table 5: Interactions of Substrates in Y143F Mutant and in Wild-Type Flavocytochrome b_2

Ppyr atoms	(A) Phenyl Pyruvate (Ppyr) subunit 1	subunit 2	distance (Å)
CB		Ala198	3.8
CD1	Ala198		3.7
CD1	Leu230		3.7
CD2	Leu286		3.7
CG		Phe143	3.7
CE1		Leu199	3.4
CE2	Phe143		3.8
CZ	heme		3.7
O1A	His373 NE2	His373 NE2	3.1/2.8
O1B	His373 NE2	His373 NE2	2.9/2.9
O1B	Tyr254 OH	Tyr254 OH	2.8/2.8
O2		Arg376 NH2	3.4
O1B	FMN N5	FMN N5	3.4/3.1
O2	FMN N5	FMN N5	4.9/4.3

Pyr atom	(B) Pyruvate (Pyr) subunit 1	subunit 2	distance (Å)
mutant Y143F			
O2	His373 NE2	Tyr254 OH	2.8/2.6
	Arg376 NE	His373 NE2	3.3/2.9
O1A	Arg289 NH2	Arg289 NH2	2.9/2.9
	Arg376 NH1	His373 NE2	2.6/2.9
		Arg376 NH2	3.2
O1B		Arg289 NH1	2.8
		Arg376 NH2	3.0
C3	FMN C4	Ala198 CB	3.7/3.6
	FMN C4α	Leu286 CD2	3.5/3.8
O2	FMN N5	FMN N5	3.6/3.1
closer to FMN	N5–C3 3.2 Å	N5–C2 3.0Å	
wild-type *S. cerevisiae*			
O2		Tyr254 OH	2.4
		His373 NE2	2.6
O1A		Arg376 NE	3.1
O1B		Tyr143 OH	2.8
C3		Leu230 CD2	3.6
O2		FMN N5	3.8
closer to FMN	C4a–O2 3.6 Å		

Ppyr and Y143F-pyr, respectively. These values are comparable to those published on the wild-type structure (9.7 Å) and on the recombinant native structure (10.6 Å). The similarity between the distance values associated with a 20-fold lower kinetic rate constant (Table 1) constitute the first experimental evidence supporting the previously proposed hypothesis that a dynamic control may be exerted over the intramolecular electron transfer rate in flavocytochorme b_2 (Miles et al., 1992; Tegoni & Cambillau, 1994a).

The Interactions between the Two Domains. The most noteworthy finding defining the role of Tyr143 concerns the interface between the two domains in the structure of Y143F complexes. In the mutant the number of interactions between the two domains is much lower than in the wild-type enzyme: four hydrogen bonds and four hydrophobic interactions in Y143F-Ppyr and four hydrogen bonds and eight hydrophobic interactions in Y143F-pyr as compared with eight hydrogen bonds and eight hydrophobic interactions in the native recombinant. Few of the contacts differ in this complex, and most of them involve Gln139; actually, this side chain, which is involved in both polar and hydrophobic interactions, has moved perceptibly during the refinement (Table 6).

The very restricted number of contacts observed in Y143F strongly supports one of the hypotheses previously put forward to explain the slow intramolecular electron transfer in this mutant. Assuming that the dynamic formation of a catalytically efficient complex between the two domains depends on the number of possible interactions at the interface, and that this number is already very small in the native proteins (thus probably limiting the rate of electron transfer), the fact that fewer interactions occur in the Y143F mutant is probably responsible for the decrease in the intramolecular electron transfer rate.

Table 6: Domains contacts in recombinant Y143F

b_2 core	FDH	distance (Å)
	(A) Y143F-phenyl Pyruvate[a]	
Asn42 OD1	Lys324 N	2.7
Leu65	Leu202	3.7
Ala67 N	Ser232 O	3.1
Tyr74	Phe325	3.4
Tyr74	Ile261	3.8
heme	Leu199	3.7
heme O1D	Lys296 NZ	3.1
heme O2D	Gln139 NE2	2.9
	(B) Y143F-pyruvate[b]	
Asn42 O	Ser323 OG	3.2
Pro44	Phe325	3.8
Leu65	Leu199	3.7
Leu65	Leu202	3.5
Ala67 N	Ser232 O	3.0
Tyr74	Phe325	3.5
Tyr74	Ile261	3.8
Pro99	Gln139	3.8
heme	Leu199	3.6
heme	Leu230	3.5
heme O1D	Gln139 NE2	2.8
heme O2D	Gln139 NE2	2.7

[a] Lacking with respect to the recombinant native: Asn42 O–Ser323 OG (3.4); Pro44–Phe325 (3.5); Ala67–Cys233 (3.8); Pro 68–Ser 234 (3.8); Tyr97 OH–Gln139 NE2 (3.1); Pro99–Leu295 (3.6); heme–Leu230 (3.8); heme O1A–Tyr143 OH (2.7). [b] Lacking with respect to the recombinant native: Asn42 OD1–Lys324 N (2.6); Ala67–Cys233 (3.8); Pro68–Ser234 (3.8); Tyr97 OH–Gln139 NE2 (3.1); heme O1A–Tyr143 OH (2.7).

CONCLUSION

On the basis of the structural analysis described above, the possibility that Tyr143 may act as an electronic wire in the electron transfer from FMN to heme through the aromatic π-electron cloud can be ruled out: although the aromatic ring occupies an identical position, the rate of electron transfer is conspicuously lower in the mutant (Miles et al., 1992). The fact that fewer interactions were observed at the interface between the domains in the Y143F mutant indicates, on the contrary, that Tyr143 is essential to the formation of the complex between the FMN and the heme domains allowing thus, but indirectly, the electron transfer. In this mutant, the loss of the Tyr143 hydrogen bond may account for the decrease in the intramolecular electron transfer rate. The presence of pyruvate and phenyl pyruvate in subunits 1 and 2 strongly suggests that the active site must be accessible in both the open and closed conformations. The flexibility of the active site is further demonstrated by the movement of the heme propionate which was hindered in the mutant structure by the phenyl ring of phenyl pyruvate. Finally, the close proximity found to exist between heme and FMN, in both the mutated and native structures, provides experimental support for the idea that the intramolecular electron transfer may be under dynamic control in flavocytochrome b_2.

ACKNOWLEDGMENT

Dr. G. Reid is kindly acknowledged for providing us with the *E. coli* clone of mutant flavocytochrome b_2. We thank Drs. S. Chapman, F. Lederer, F. S. Mathews, and G. Reidfor fruitful discussions. We thank Dr. S. Ottonello's group for their kind assistance with the cell culture.

REFERENCES

Baudras, A. (1962) *Biochem. Biophys. Res. Commun. 7*, 310−314.

Baudras, A. (1972) in *Dynamic Aspect of Conformation Changes in Biological Macromolecules* (Sadron C., Ed.) pp 181−205, D. Reidel, Dordrecht, The Netherlands.

Black, M. T., White, S. A., Reid, G. A., & Chapman, S. K. (1989) *Biochem. J. 258*, 255−259.

Brünger, A. T. (1988) in *Crystallographic Computing 4: Techniques and New Technologies* (Isaacs, N. W., Taylor, M. R., Eds.) pp 126−140, Clarendon Press, Oxford.

Capeillère-Blandin, C. (1982) *Eur. J. Biochem. 128*, 533−542.

Capeillère-Blandin, C., Bray, R., Iwatsubo, M., & Labeyrie, F. (1975) *Eur. J. Biochem. 54*, 549−566.

Dubois, J., Chapman, S. K., Mathews, F. S., Reid, G. A., & Lederer, F. (1990) *Biochemistry 29*, 6393−6400.

Guiard, B. (1985) *EMBO J. 4*, 3265−3272.

Guiard, B., Groudinsky, O., & Lederer, F. (1974) *Proc. Natl. Acad. Sci. U.S.A. 71*, 2539−2543.

Iwatsubo, M., Mevel-Ninio, M., & Labeyrie, F. (1977) *Biochemistry 16*, 3558−3566.

Jacq, C., & Lederer, F. (1974) *Eur. J. Biochem. 41*, 311−320.

Labeyrie, F. (1982) in *Flavins and Flavoproteins* (Massey, V., & Williams, C. H., Eds.) pp 823−832, Elsevier North Holland Inc., Amsterdam.

Labeyrie, F., Baudras, A., & Lederer, F. (1978) *Methods Enzymol. 53*, 238−256.

Lederer, F. (1992) *Protein Sci. 1*, 540−548.

Lederer, F., & Mathews, F. S. (1987) in *Flavins and Flavoproteins* (Edmondson, D. E., & McCormick, D. B., Eds.) pp 133−142, Walter de Gruyter, New York.

Miles, C. S., Rouvière-Fourmy, N., Lederer, F., Mathews, F. S., Reid, G. A., Black, M. T., & Chapman, S. K. (1992) *Biochem. J. 285*, 187−192.

Morris, A. L., MacArthur, M. W., Hutchinson, E. G., & Thornton, J. M. (1992) *Proteins 12*, 345−364.

Pajot, P., & Claisse, M. (1974) *Eur. J. Biochem. 49*, 275−285.

Pompon, D., Iwatsubo, M., & Lederer, F. (1980) *Eur. J. Biochem. 104*, 479−488.

Reid, G. A., White, S. A., Black, M. T., Lederer, F., Mathews, F. S., & Chapman, S. K. (1988) *Eur. J. Biochem. 178*, 329−333.

Roussel, A., & Cambillau, C. (1991) in *Silicon Graphics Geometry Partners Directory* (Silicon Graphics, Ed.) p 86.

Rouvière-Fourmy, N., Capeillère-Blandin, C., & Lederer, F. (1994) *Biochemistry 33*, 798−806.

Tegoni, M., & Cambillau, C. (1994a) *Protein Sci. 3*, 303−314.

Tegoni, M. & Cambillau, C. (1994b) *Biochimie 76*, 501−514.

Tegoni, M., Silvestrini, M. C., Labeyrie, F., & Brunori, M. (1984) *Eur. J. Biochem. 140*, 39−45.

Tegoni, M, Janot, J. M., & Labeyrie, F. (1986) *Eur. J. Biochem. 155*, 491−503.

Xia, Z. X., & Mathews, F. S. (1990) *J. Mol. Biol. 212*, 837−863.

Xia, Z. X., Shamala, N., Bethge, P. H., Lim, L. W., Bellamy, H. D., Xuong, Ng.-h., Lederer, F., & Mathews, F. S. (1987) *Proc. Natl. Acad. Sci. U.S.A. 84*, 2629−2633.

BI950329A